Mercury Removal From Coal Combustion Flue Gas by Pyrite-Modified Fly Ash Adsorbent

Liqiang QI (qiliqiang@ncepu.edu.cn)
North China Electric Power University https://orcid.org/0000-0001-6039-1224
Xu WANG
North China Electric Power University
Wen WANG
North China Electric Power University
Jingxin LI
North China Electric Power University
Yan HUANG
North China Electric Power University

Research Article

Keywords: fly ash, pyrit, modified, Hg0 removal

Posted Date: October 26th, 2021

DOI: https://doi.org/10.21203/rs.3.rs-934628/v1

Version of Record: A version of this preprint was published at Environmental Science and Pollution Research on January 31st, 2022. See the published version at https://doi.org/10.1007/s11356-022-18963-z.

Abstract

Pyrite and fly ash have certain advantages in adsorption and mercury oxidation. The pyrite-modified fly ash (PY+AC-FA) mercury adsorbent was prepared by mixing pyrite (PY) with acid-modified fly ash (AC-FA), which has better mercury removal effect than AC-FA. The experimental results of mercury adsorption show: when the reaction temperature is 50°C, the best doping proportion of modified fly ash is 20wt%, the mass proportion of pyrite to acid modified fly ash is 4:1, and the flue gas flow rate is 1.0L/min, the adsorbent has the best performance, and the adsorption rate of mercury reaches 91.92%. BET, XRD, SEM, TG-DSG and XRF were used to characterize these adsorbents. And the mechanism of mercury removal of pyrite-modified fly ash adsorbent is inferred: Hg^0 is first adsorbed on the surface of the adsorbent, and then oxidized to HgS by the active component FeS_2 in pyrite-modified fly ash.

1. Introduction

Coal-fired power plants emit large amounts of mercury during coal combustion(Pirrone et al., 2010). Mercury has high toxicity, non-degradability and bioaccumulation, which can pose a great threat to human health and the ecological environment(Lin et al., 2014). Therefore, it is important to reduce mercury emissions from coal-fired power plants.

Post-combustion mercury removal technology is the mainstream technology at present. There are two kinds of mercury removal technologies after combustion: One is to spray activated carbon or other kinds of solid adsorbent to remove mercury(Olson et al., 2000; Presto and Granite, 2006); The other is the oxidation of mercury through catalysts in denitration equipment. Oxidized mercury is absorbed by wet desulfurization equipment(Yang et al., 2016; Luo et al., 2010; Zhou et al.,2016; Li et al., 2015; Li et al., 2018). Han et al. (2016) modified the activated carbon by Pd doping, Pd and Fe co-doping. The experimental results showed that the modified activated carbon adsorbent could reached more than 92% efficiency of mercury removal under the experimental condition at 200°C, and could operate stably for 6h. However, the cost of this method is relatively high, and the application in practice needs to reduce the operating cost by recycling. As one of the adsorbents for mercury removal, fly ash has the advantages of wide source and low price, which makes it have a large market in practical application(Wang and Wu, 2006). The fly ash consists of inorganic components and organic components. The inorganic components account for about 98%, mainly including aluminosilicates, silicates, sulfates, calcium oxide and iron oxides. The organic components are mainly unburned carbon, which has a great influence on the efficiency of mercury removal from fly ash(Xia et al., 2015). Xu et al. (2013) showed that the main mechanism of mercury removal from fly ash was physical and chemical adsorption. The high specific surface area, small pore size structure and incomplete combustion of carbon make the fly ash have unique adsorption activity for mercury removal. Tian et al. (2017) used NaCl and NaBr for loading modification of coal-fired power plant fly ash. The results showed that the adsorbent modified with 5% NaCl solution for 3 hours has a better performance of mercury removal. Under certain temperature conditions, the efficiency of mercury removal was above 85%, with the highest being 92.6%. Thus, fly ash can be used as a cost-effective alternative to activated carbon. However, fly ash has limited adsorption

ability, which has to be improved through modification methods. Pyrite is a sulfide mineral rich in nature, containing a large amount of Fe and S elements(Duan et al., 2016; Han et al., 2014). The reduced sulfur ligand is prone to complexation by mercury, resulting in the formation of insoluble and potentially less dangerous HgS(Sun et al., 2017; Stein etal., 1996; Willet et al., 1992).

In this study, pyrite-modified fly ash (PY+AC-FA) adsorbent with good performance of mercury removal was prepared by doping the modified fly ash with pyrite. The effects of the modification method, reaction temperature, nitrogen flow rate and doping proportion of fly ash were investigated. BET, SEM, XRD, XRF and TG-DSC were used to characterize the internal structure and the mechanism of mercury removal, which provided a new idea for the adsorption of mercury from fly ash.

2. Methods And Materials

2.1 Adsorption performance evaluation system

In order to evaluate the adsorbent performance, a fixed bed reactor was constructed as shown in Fig. 1. A series of experiments were conducted to investigate the performance of various adsorbents and the mechanism of mercury removal. The fixed bed reaction system consists of three main components: the mercury vapor generation unit, fixed bed reaction unit and tail gas treatment unit. Because of the instability of pyrite in air(Bower et al., 2008), N_2 was used as the carrier gas throughout the experiment. The experimental pipeline was connected by PTFE tube, and the entire pipeline was wrapped with heating cable to prevent the mercury from liquefying and remaining in the pipeline.

The mercury vapor is emitted from the mercury permeable tube in the U-shaped tube. When the external temperature is constant, the mercury in the U-shaped tube reaches vapor-liquid equilibrium, and the mercury vapor steadily escapes at a certain rate, and then is blown into the gas path by N_2. Therefore, the experiment can control the initial mercury concentration by changing the water bath temperature and nitrogen flow rate. The fixed bed reactor in this experiment is composed of a quartz reaction tube and a temperature-controlled heating tape. To prevent leakage during aeration, the adsorbent is placed between two layers of glass wool. In this experiment, $KMnO_4/H_2SO_4$ absorption method(Wang et al., 2013) was used to determine the concentration of Hg^0. After the reaction, the tail gas may contain a certain amount of mercury, and the tail gas needs to pass through the first acidic potassium permanganate absorption bottle and then through the activated carbon adsorption treatment, and finally be collected by the tail gas treatment device.

2.2 Materials

Reagents: Sulfuric acid (H_2SO_4), hydrochloric acid (HCl), nitric acid (HNO_3), potassium permanganate ($KMnO_4$) and stannous chloride ($SnCl_2$) were all analytical reagent.

Instruments:The BET of the adsorbents was determined by Quadrasorb EVO^{TM}. The specific surface area, pore volume and pore size distribution of the material to be measured were determined by nitrogen physical adsorption method. the microstructure of adsorbents were characterized by scanning electron microscopy(SEM). The crystal structure of adsorbents were determined by X-ray diffraction spectroscopy (XRD). The element composition of adsorbents were determined by X-ray fluorescence probe (XRF). The thermogravimetric analysis (TG-DSC) instrument model is STA-8000 to analyze the adsorbents on the reacted material.

X-ray fluorescence spectrometer (XRF) is used to analyze the chemical composition of fly ash and pyrite, as shown in Table 1.

2.3 Adsorbents preparation

The fly ash used in this experiment is taken from a power plant in North China, marked as FA. Weigh an appropriate amount of FA into a conical flask, add H_2SO_4 or NaOH and stir for half an hour at 25°C. After filtration and drying, acid-modified fly ash (AC-FA) or alkali-modified fly ash (AL-FA) was obtained.

The group with better mercury removal performance in AC-FA and AL-FA was selected to be doped with pyrite (PY), and the effects of FA doping amount, reaction temperature, doping proportion and carrier gas flow rate on mercury removal performance were investigated.

Table 1 Chemical composition of fly ash and pyrite (wt%)

composition	fly ash	pyrite
SiO_2	49.23	2.758
Al_2O_3	35.642	1.006
Fe_2O_3	5.108	36.951
CaO	3.074	0.319
TiO_2	1.852	——
P_2O_5	1.166	0.449
SO_3	1.907	56.895
K_2O	1.197	——
Na_2O	0.097	0.308
MgO	0.235	0.369

2.4 Adsorption performance experiment

Before starting the experiment, turn on the fume hood, mercury analyzer, water bath and heat belt for preheating. The adsorbent is placed in the reactor with the glass wool. The mercury concentration in the $H_2SO_4/KMnO_4$ solution in this experiment was measured. Each sample was measured three times to take its average value. After the overall experiment, the ventilation should be stopped first, the U-shaped tube was remove, and then the lower wall of the mercury permeation tube was separate from the glass beads. The mercury permeation tube should be removed after cooling.

The mercury removal efficiency was measured by the concentration of mercury before and after the reaction. The mercury concentration is determined by the absorbance of the sample. The mercury removal efficiency of the adsorbent was measured according to the following equation Eq.(1):

$$\eta = \frac{Hg_{in} - Hg_{out}}{Hg_{in}} \times 100\% \quad (1)$$

Where, Hg_{in}-initial concentration of gaseous elemental mercury, μg/L; Hg_{out}-concentration of gaseous elemental mercury after adsorption, μg/L; η-Mercury removal efficiency, %.

3. Results And Discussions

3.1 Mercury removal performance of modified fly ash

Fig. 2 shows the mercury removal efficiency of FA, AC-FA, AL-FA, PY and PY+AC-FA. It can be seen from Fig. 2 that the mercury removal efficiency of adsorbent decreases with the increase of time. Compared with AL-FA, the mercury removal efficiency of AC-FA is higher. The mercury removal efficiency of AC-FA reaches 63.37% at 10min, while that of AL-FA is 52.09%. The efficiency of FA reaches 45.85% at 10min, indicats that the modification method with acid and alkali beneficial to the removal of mercury.

PY+AC-FA is prepared by mixing AC-FA and PY in a certain proportion. Compared with AC-FA and PY, PY+AC-FA offers greater improvements in mercury removal efficiency and persistence, especially the persistence. The mercury removal efficiency of the pyrite adsorbent doped with AC-FA increass from 74.39% to 84.70% at 10min. After 10min, PY+AC-FA could still maintain about 75% of the mercury removal efficiency, and the efficiency could last until 30min. The reason for the better adsorption performance of PY+ AC-FA is that PY+ AC-FA has a large specific surface area according to the BET and SEM characterization in 3.3.1 and 3.3.2. Such a structure is favorable for the adsorption capacity. On the other hand, the FeS_2 in PY+AC-FA is chemically adsorbed with mercury in simulated flue gas based on XRD characterization in 3.3.3.

The modification can improve the adsorption efficiency of FA to a certain extent. In the subsequent experiments, PY+AC-FA were mixed for the experiment.

3.2 Mercury removal performance of PY+AC-FA

3.2.1 Effect of reaction temperature on adsorbent

As shown in Fig. 3, in the experimental temperature range (50-110°C), the mercury removal efficiency of PY+AC-FA decreases with increasing reaction temperature. The mercury removal efficiency of PY+AC-FA is maintained at a high level from 50°C to 90°C. After the experimental temperature exceeded 90°C, the mercury removal efficiency decreases significantly. The effect of reaction temperature on the Hg^0 removal by the adsorbent is mainly manifested in two aspects: on the one hand, the increase of temperature will promote the removal of Hg^0 from the surface of PY+AC-FA, so that Hg^0 will be carried away by nitrogen before it is oxidized; On the other hand, higher temperature can improve the activity of PY+AC-FA(Li et al., 2018), but as the temperature continues to increase, it will cause the release of elemental sulfur from PY+AC-FA, resulting in lower removal efficiency.

3.2.2 Effect of nitrogen flow rate on adsorbent

The flow rate of nitrogen has three main effects on the efficiency of mercury removal: the concentration of imported mercury, the reaction time of Hg0 with the adsorbent, and the driving force of nitrogen in the adsorption process. With the increase of flow rate, the gas driving force will increase, and the reaction time between adsorbent and Hg^0 will decrease. Hsi et al. (2001) that the higher the imported mercury concentration, the more active sites and empty spaces are required for adsorption. Therefore, the relative adsorption space and active sites in the adsorbent are reduced, which leads to a decrease in the efficiency of mercury removal As shown in Fig. 4, the mercury removal efficiency reaches the highest when the nitrogen flow rate is 1.0L/min. The driving force of the flow rate is the main factor affecting the adsorption when the flow rate is small. However, when the flow rate is too high, the decrease of reaction time and the increasing concentration of mercury become the dominant factors, which reduces the performance of the adsorbent in removing mercury.

3.2.3 Effect of AC-FA doping proportion on adsorbent

In order to investigate the effect of the percentage of AC-FA on the efficiency of the adsorbent, PY+AC-FA adsorbents with modified fly ash percentages of 20wt%, 25wt%, 33.3wt%, 50wt%, 66.7wt%, 75wt% and 80wt% were prepared, respectively. The variation of mercury adsorption efficiency with the proportion of AC-FA is shown in Fig. 5.

As shown in Fig. 5, when the proportion of AC-FA is 0, the mercury removal efficiency of PY+AC-FA is 74.39%. With the increase of the proportion, the mercury removal performance of adsorbent is greatly

improved to 91.92%. However, when the proportion of AC-FA is more than 20wt%, the mercury removal efficiency decreases from 91.92% to 59.1%. When the proportion of AC-FA is less than 20wt%, the incorporation of AC-FA will increase the specific surface area of PY+AC-FA and enhance its physical adsorption capacity. However, with the increase of the AC-FA proportion, the pyrite content decreases and the adsorbent surface mainly undergoes physical adsorption, which is not sufficient to remove mercury from the flue gas, thus leading to a gradual decrease in the efficiency of mercury removal.

3.3 Characterization results and discussion

3.3.1 BET

The BET characterization results are shown in Table 2.

Table 2 Specific surface area of samples

Sample	the doping proportion of AC-FA (%)	Specific surface area (m^2/g)	Pore volume (cc/g)	Average pore size (nm)
FA	——	1.610	0.004	4.737
AC-FA	——	2.612	0.008	4.168
AL-FA	——	3.969	0.010	4.435
PY	——	0.953	0.003	4.173
PY_4+AC-FA_1	20.00	6.276	0.011	2.523
PY_2+AC-FA_1	33.33	2.850	0.008	4.181
PY_1+AC-FA_1	50.00	3.028	0.007	4.171
PY_1+AC-FA_3	75.00	3.275	0.005	2.126

As can be seen from Table 2, the specific surface area of FA whice modified by acid and alkali increases by about 162% and 247%. The maximum specific surface area of PY doped with AC-FA is 6.276.The specific surface area of AC-FA doped 20 wt% is increases by 220% compared to AC-FA doped 33.33 wt%. However, the experimental results in 3.2.3 shows that the efficiency of mercury removal is 91.93% and 91.38% for PY_4+AC-FA_1 and PY_2+AC-FA_1, respectively. The results of Li et al. (2018) showed that an

excessive specific surface area increases the desorption reaction of the adsorbent, which leads to a decrease in the removal efficiency of pollutants.

3.3.2 SEM

Fig. 6(a-e)shows SEM images of FA, AC-FA, AL-FA, PY and PY+AC-FA with different doping proportions at 500 and 2000 times magnification. As can be seen from the Fig. 6 (a-c), FA agglomerates have various morphological types, most of the particles are spherical, while a few of them are massive or irregular. The surface roughness and pore size of AC-FA and AL-FA are increased, and the pore size of AL-FA particles is larger, which is consistent with the BET measurement results in 3.3.1. From Fig. 6(d-e), it can be seen that the surface of PY+AC-FA is rougher, the pores between the granules increase, and the pore diameter increases after the doping of AC-FA. Compared to FA, PY+AC-FA has larger pores and pore size than FA. The SEM images at 2000 times shows some particles attached to the surface of PY+AC-FA. To determine whether these particles are loaded thionite, the adsorbent is further characterized and analyzed.

3.3.3 XRD

The XRD patterns show the differences between the FA samples before and after the processing. It can be seen from Fig. 7 that the diffraction peaks of FA before and after modification are many and complex. The peaks marked in the Fig. 7 are the diffraction peaks of mullite (AS), followed by quartzand other substances(Li et al., 2017). By comparison, there is little difference before and after modification except diffraction peak. The peak of modified fly ash is narrower and sharper, and the peak width is smaller.

According to Scheerrer formula($\beta = 0.89\lambda/Dcos\theta$,where λ is thex-ray wavelength, D is the average crystal size.), the particle size of modified fly ash is smaller and has a larger specific surface area, which is also consistent with the BET measurement results in 3.3.1. It can be seen that sulfuric acid and sodium hydroxide only change the physical structure of the surface of FA, and the overall crystal and material structure of FA do not change.

As can be seen from Fig. 8, the main diffraction peaks of the PY+AC-FA are mullite and FeS_2. The diffraction peak response values of mullite and FeS_2 change with the proportion of AC-FA, which is consistent with the actual situation.

The adsorbents before and after the adsorption reaction are analyzed by XRD to study the reaction mechanism of PY+AC-FA removal of mercury. Fig. 9 shows the comparison results.

It can be seen from Fig. 9 that the diffraction peak types of PY+AC-FA before and after the reaction are basically unchanged, and only the diffraction peaks of FeS_2 is different. The intensity of FeS_2 diffraction peaks of PY+AC-FA after the reaction is obviously weaker than that before the reaction. To make the comparison more obvious, the two images are overlapped on the same baseline. As shown in Fig. 9, the response value of the FeS_2 diffraction peaks of PY+AC-FA before the reaction is higher than that after the

reaction, which indicates that FeS_2 is involved in the reaction and is consumed by reduction in the process of mercury removal(Dyrssen and Wedborg, 1991; Yang et al., 2018).

3.3.4 TG-DSC

TG-DSC characterization verified that FeS_2 in PY+AC-FA is reduced and consumed in the process of mercury removal. Fig. 10 shows the TG-DSC pattrens of PY+AC-FA when heated at various temperatures up to 800°C. As shown in Fig. 10, the weight loss peak of surface adsorbed water on PY+AC-FA appeared between 27°C and 110°C. As the temperature increases, the weight dropped slowly and finally reaches 15.213mg at 420°C. This indicates that Hg^0 (ad) adsorbing on the surface of PY+AC-FA begins to evaporate above its boiling point. The pattern decreases significantly after 420°C, indicates that PY+AC-FA began to lose weight substantially. This can be interpreted as the chemical adsorption of FeS_2 in PY+AC-FA with Hg^0 produces HgS(Li et al., 2017; Liao et al., 2016; Yang et al., 2018; Zhao et al., 2016; Wu et al., 2008; Bhargava et al., 2009), and when the temperature is higher than 420°C, HgS starts to decompose into Hg and S(Yang et al., 2017). Therefore, the TG-DSC analysis indicates that PY+AC-FA contains surface adsorbed water, Hg, and HgS.

Based on the BET, SEM, XRF, XRD, TG-DSC characterization of adsorbents., the Hg^0 removal mechanism is proposed, as shown in Eq.(2)-(4).

Firstly, Hg^0 is adsorbed on the surface of the adsorbent,

$$Hg_g^0 + (\mathrm{PY} + \mathrm{AC} - \mathrm{FA}) \rightarrow Hg_{ad}^0 \quad (2)$$

Secondly, Hg^0 reacts with the active component FeS_2 in PY+AC-FA,

$$Hg_{ad}^0 + FeS_2 \rightarrow HgS_{ad} + FeS \quad (3)$$

$$Hg_{ad}^0 + FeS \rightarrow HgS_{ad} + Fe \quad (4)$$

Finally, most of the mercury is adsorbed on the surface of the adsorbent as HgS.

4. Conclusion

In this paper, the sulfuric acid modified fly ash (AC-FA) was mixed with pyrite (PY), and the pyrite-modified fly ash (PY+AC-FA) adsorbent for mercury removal was successfully prepared. The characterizations results shows that PY+AC-FA has large specific surface area, pore diameter and successfully loaded FeS_2 on the surface. When the reaction temperature is 50°C, the doping proportion of AC-FA is 20wt%, and the nitrogen flow rate is 1.0L/min, the removal rate of Hg^0 can reach 91.92%.

By characterization analysis of the adsorbents, and XRD results of PY+AC-FA before and after the reaction.Based on the BET, SEM, XRF, XRD, TG-DSC characterization of adsorbents. The mercury removal mechanism of pyrite-modified fly ash (PY+AC-FA) was proposed:First, Hg^0 was adsorbed on the surface of the adsorbents, then Hg^0 was oxidized by the active component FeS_2 in pyrite - modified fly ash (PY+AC-FA) to HgS, and finally most of the mercury was adsorbed on the surface of the adsorbents in the form of HgS.

Declarations

- **Ethics approval and consent to participate**

Not applicable.

- **Consent for publication**

Not applicable.

- **Availability of data and materials**

Not applicable.

- **Competing interests**

The authors declare that they have no competing interests.

- **Funding**

This work was supported by the Natural Science Foundation of Hebei Province (Grant No. B2019502067) and the Fundamental Research Funds for the Central Universities (Grant No. 2020MS152).

- **Authors' contributions**

All authors contributed to the study conception and design. Material preparation, data collection and analysis were performed byWen WANG, Jingxin LI and Yan HUANG. The first draft of the manuscript was written by Xu WANG and Liqiang QI, and all authors commented on previous versions of the manuscript. All authors read and approved the final manuscript.

Acknowledgment

This work was supported by the Natural Science Foundation of Hebei Province (Grant No. B2019502067) and the Fundamental Research Funds for the Central Universities (Grant No. 2020MS152).

References

1. Bhargava, S.K., Garg, A., Subasinghe, N.D., 2009. In situ high-temperature phase transformation studies on pyrite. Fuel. 88, 988–993. DOI:10.1016/j.fuel.2008.12.005.
2. Bower, J., Savage, K.S., Weinman, B., Barnett, M.O., Hamilton, W.P., Harper, W.F., 2008. Immobilization of mercury by pyrite (FeS_2). Environ. Pollut. 156, 504-516. DOI:10.1016/j.envpol.2008.01.011.
3. Duan, Y.H., Han, D.S., Batchelor, B., Abdel-Wahab, A., 2016. Synthesis, characterization, and application of pyrite for removal of mercury. Colloids Surf., A. 490, 326-335. DOI:10.1016/j.colsurfa.2015.11.057.
4. Dyrssen, D., Wedborg, M., 1991. The sulphur-mercury(II) system in natural waters. Water, Air, Soil Pollut. 56, 507–509. DOI:10.1007/BF00342295.
5. Han, D.S., Orillano, M., Khodary, A., Duan, Y.H., Batchelor, B., Abdel-Wahab, A., 2014. Reactive iron sulfide (FeS)-supported ultrafiltration for removal of mercury (Hg(II)) from water. Water. Res. 53, 310–321. DOI:10.1016/j.watres.2014.01.033.
6. Han, L.N., He, X.X., Yue, C.X., Hu, Y.F., Li, L.N., Chang, L.P., Wang, H., Wang, J.C., 2016. Fe doping Pd/AC sorbent efficiently improving the Hg^0 removal from the coal-derived fuel gas. Fuel. 182, 64-72. DOI:10.1016/j.fuel.2016.05.046.
7. Hsi, H.C., Rood, M.J., Rostam-Abadiet, M., Chen, S., Chang, R., 2001. Effects of sulfur impregnation temperature on the properties and mercury adsorption capacities of activated carbon fibers (ACFs). Environ. Sci. Technol. 35, 2785–2791. DOI:10.1021/es001794k.
8. Li, H.L., Wu, S.K., Wu, C.Y., Wang, J., Li, L.Q., Shih, K., 2015. SCR atmosphere induced reduction of oxidized mercury over CuO-CeO_2/TiO_2 catalyst. Environ. Sci. Technol. 49, 7373–7379. DOI:10.1021/acs.est.5b01104.
9. Li, H.L., Zhao, J.X., Zhang, W.L., Yang, J.P., Wang, J., Zhang, M.G., Yang, Z.Q., Li, L.Q., Shih, K., 2018. NH_3 inhibits mercury oxidation over low-temperature MnO_x/TiO_2 SCR catalyst. Fuel Process. Technol. 176, 124–130. DOI:10.1016/j.fuproc.2018.03.022.
10. Li, H.L., Zhu, L., Wang, J., Li, L.Q., Lee, P.H., Feng, Y., Shih, K., 2017. Effect of nitrogen oxides on elemental mercury removal by nanosized mineral sulfide. Environ. Sci. Technol. 51, 8530–8536. DOI:10.1021/acs.est.7b00224.
11. Li, H.L., Zhu, W.B., Yang, J.P., Zhang, M.G., Zhao, J.X., Qu, W.Q., 2018. Sulfur abundant S/FeS_2 for efficient removal of mercury from coal-fired power plants. Fuel. 232,476-484. DOI:10.1016/j.fuel.2018.06.002.
12. Li, J.J., Zhu, J.B, Qiao, S.Y., Yu, Z.W., Wang, X.L., Liu, Y., Meng, X.R., 2017. Processing of coal fly ash magnetic spheres for clay water flocculation. Int. J. Miner. Process. 169, 162-167. DOI:10.1016/j.minpro.2017.11.006.
13. Liao, Y., Chen, D., Zou, S.J. Xiong, S.C., Xiao, X., Dang, H., Chen, T.H., Yang, S.J., 2016. Recyclable naturally derived magnetic pyrrhotite for elemental mercury recovery from flue gas. Environ. Sci. Technol. 50, 10562–10569. DOI:10.1021/acs.est.6b03288.

14. Lin, G.X., Penner, J.E., Clack, H.L., 2014. Radiative forcing associated with particulate carbon emissions resulting from the use of mercury control technology. Environ. Sci. Technol. 48, 10519–10523. DOI:10.1021/es502382h.
15. Luo, G.Q., Yao, H., Xu, M.H., Gupta, R., Xu, Z.H., 2010. Identifying modes of occurrence of mercury in coal by temperature programmed pyrolysis. Proc. Combust. Inst. 33, 2763–2769. DOI:10.1016/j.proci.2010.06.108.
16. Olson, E.S., Miller, S.J., Sharma, R.K., Dunham, G.E., Benson, S.A., 2000. Catalytic effects of carbon sorbents for mercury capture. J. Hazard. Mater. 74, 61–79. DOI:10.1016/S0304-3894(99)00199-5.
17. Pirrone, N., Cinnirella, S., Feng, X., Finkelman, R.B., Friedli, H.R., Leaner, J., Mason, R., Mukherjee, A.B., Stracher, G.B., Streets, D.G., Telmer, K., 2010. Global mercury emissions to the atmosphere from anthropogenic and natural sources. Atmos. Chem. Phys. 10, 5951–5964. DOI:10.5194/acp-10-5951-2010.
18. Presto, A.A., Granite, E.J., 2006. Survey of catalysts for oxidation of mercury in flue gas. Environ. Sci. Technol. 40, 5601-5609. DOI:10.1021/es060504i.
19. Stein, E.D., Cohen, Y., Winer, A.M., 1996. Environmental distribution and transformation of mercury compounds. Crit. Rev. Env. Sci. Technol. 26, 1-43. DOI: 10.1080/10643389609388485.
20. Sun, Y., Lou, Z.M., Yu, J.B., Zhou, X.X., Lv, D., Zhou, J.S., Baig, S.A., Xu, X.H., Immobilization of mercury(II) from aqueous solution using Al_2O_3-supported nanoscale FeS. Chem. Eng. J. 323, 483-491. DOI:10.1016/j.cej.2017.04.095.
21. Tian, Y.M., Liu, Q.C., Kong, M., Zhao, D., Yang, J., Ren, S., 2017. Preparation and performance analysis of modified fly ash-based mercury removal adsorbent. Techniques and Equipment for Environmental Pollution Control. 11, 4751-4756. DOI:10.12030 /j.cjee.201604037.
22. Wang, S.B., Wu, H.W., 2006. Environmental-benign utilisation of fly ash as low-cost adsorbents. J. Hazard. Mater. 136, 482-501. DOI:10.1016/j.jhazmat.2006.01.067.
23. Wang, X.F., Deng, S., Liu, Y., Zhang, F., Zhang, C., Cao, Q., 2013. Experimental Study on Ontario Mercury Testing Method in Coal-fired Flue Gas. Environmental Engineering. 31, 126-131. DOI:10.13205/j.hjgc.201302032.
24. Willet, K.L., Turner, R.R., Beauchamp, J.J., 1992. Effect of chemical form of mercury on the performance of dosed soils in standard leaching protocols: EP and TCLP. Hazard. Waste Hazard. Mater. 9, 275-288. DOI:10.1089/hwm.1992.9.275.
25. Wu, S.J., Ozaki, M., Uddin, M., Sasaoka, E., 2008. Development of iron-based sorbents for Hg^0 removal from coal derived fuel gas: Effect of hydrogen chloride. Fuel. 87, 467–474. DOI:10.1016/j.fuel.2007.06.016.
26. Xia, W.Q., Huang, Y.J., Li, M., 2015. Research progress of coal-fired mercury removal technology. Energy Research and Utilization. 6, 24-29. DOI:10.16404/j.cnki.issn1001-5523.2015.06.011.
27. Xu, W.Q., Wang, H., Zhu, T.Y., Kuang, J.Y., Jing, P.F., 2013. Mercury removal from coal combustion flue gas by modified fly ash. J. Environ. Sci. 25, 393-398. DOI:10.1016/S1001-0742(12)60065-5.

28. Yang, J.P., Ma, S.M., Zhao, Y.C., Zhang, J.Y., Liu, Z.H., Zhang, S.H., Zhang, Y., Liu, Y.M., Feng, Y.X., Xu, K., Xiang, J., Zheng, C.G., 2017. Mercury emission and speciation in fly ash from a 35 MWth large pilot boiler of oxyfuel combustion with different flue gas recycle. Fuel. 195, 174-181. DOI:10.1016/j.fuel.2017.01.036.
29. Yang, Y., Liu, J., Shen, F., Zhao, L., Wang, Z., Long, Y., 2016. Kinetic study of heterogeneous mercury oxidation by HCl on fly ash surface in coal-fired flue gas. Combust. Flame. 168, 1–9. DOI:0.1016/j.combustflame.2016.03.022.
30. Yang, Y.j., Liu, J., Liu, F., Wang, Z., Miao, S., 2018. Molecular-level insights into mercury removal mechanism by pyrite. J. Hazard. Mater. 344, 104–112. DOI:10.1016/j.jhazmat.2017.10.011.
31. Zhao, H.T., Yang, G., Gao, X., Pang, C.H., Kingman, S.W., Wu, T., 2016. Hg^0 capture over CoMoS/gamma-Al_2O_3 with MoS_2 nanosheets at low temperatures. Environ. Sci. Technol. 50, 1056–1064. DOI:10.1021/acs.est.5b04278.
32. Zhou, Z.J., Liu, X.W., Zhao, B., Shao, H.Z., Xu, Y.S., Xu, M.H., 2016. Elemental mercury oxidation over manganese-based perovskite-type catalyst at low temperature. Chem. Eng. J. 288, 701–710. DOI:10.1016/j.cej.2015.12.057.

Figures

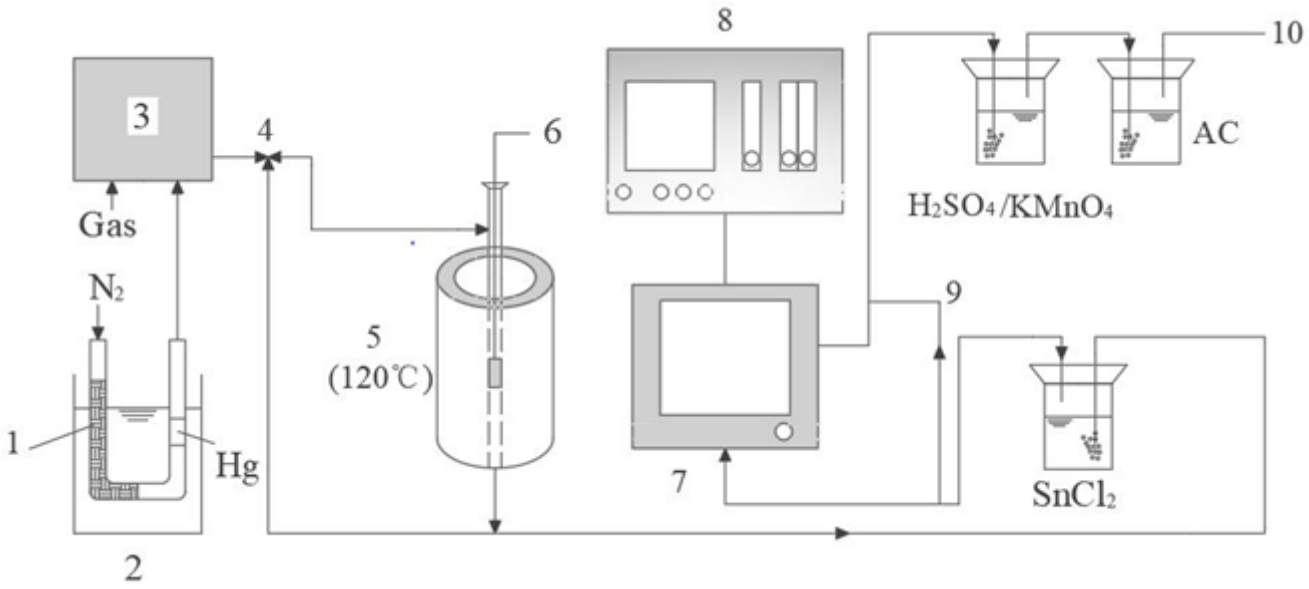

Figure 1

Fixed bed reactor. 1-mercury permeation tube; 2-water bath; 3-mixer; 4-three-way valve; 5-reactor; 6-thermocouple; 7-computer; 8-mercury meter; 9-pressure reducing valve; 10-exhaust gas collector.

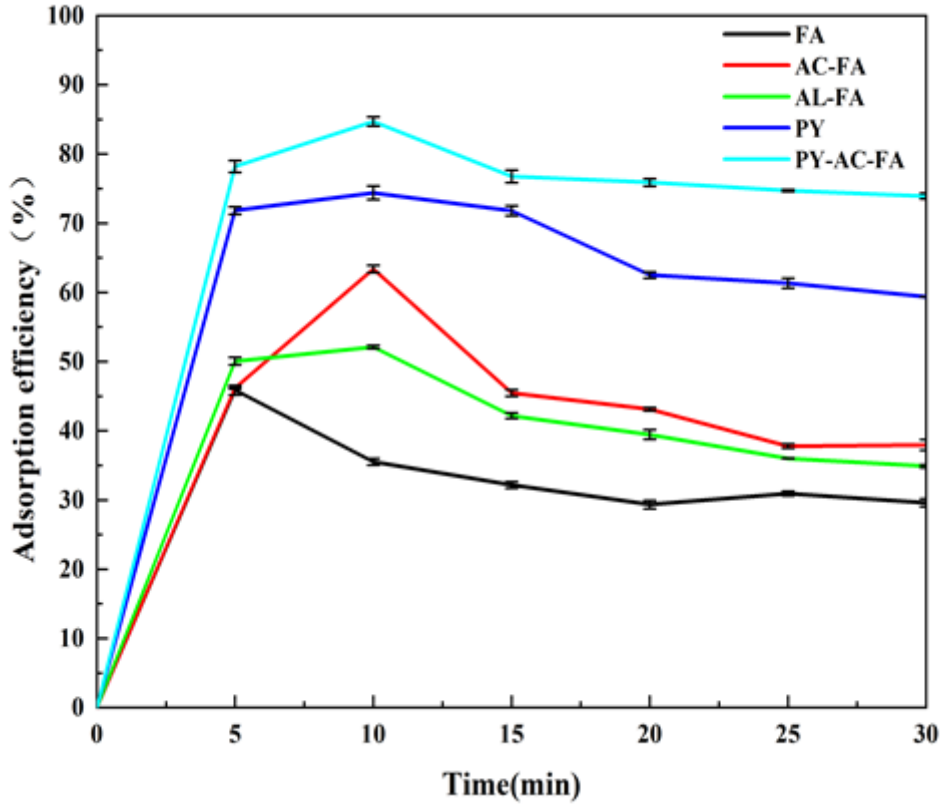

Figure 2

Adsorption efficiency of modified fly ash

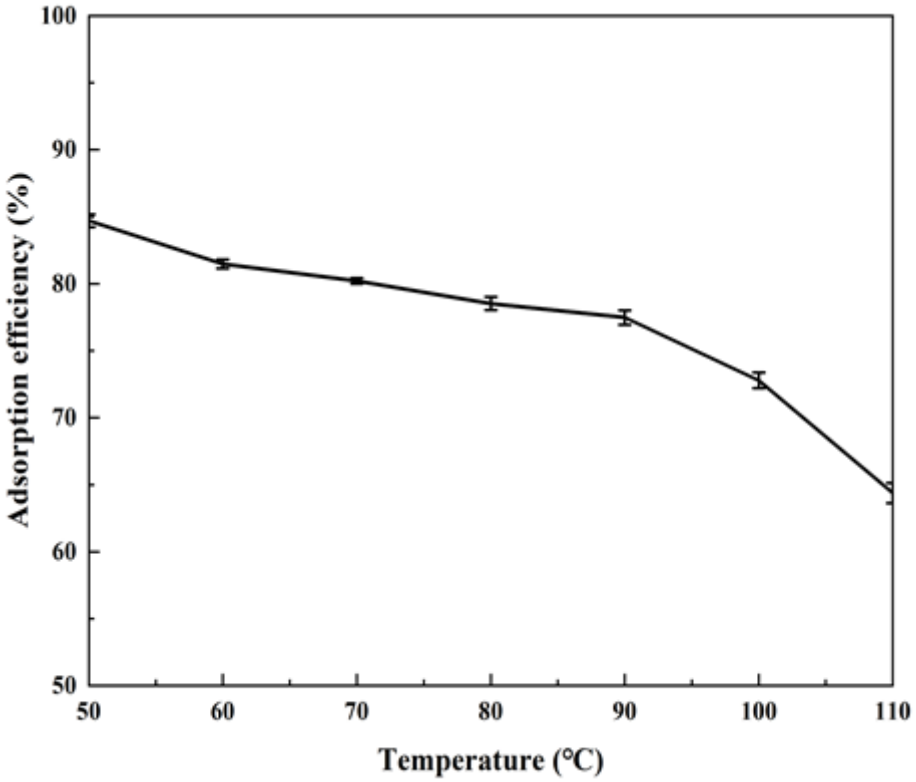

Figure 3

Effect of reaction temperature on the activity of adsorbent. Reaction conditions: the nitrogen flow rate is 1.2L/min; the mercury permeation tube water bath temperature is 60°C; the reaction time is 10min; the mass proportion of AC-FA and PY is 1:1.

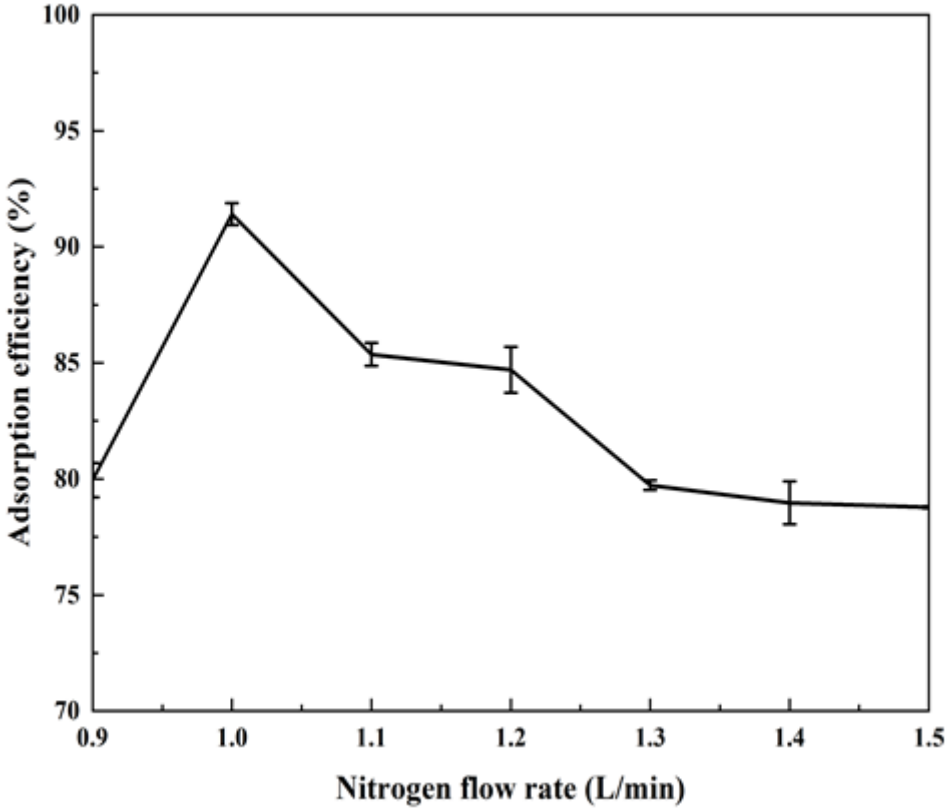

Figure 4

Effects of nitrogen flow rate. Reaction conditions: the mercury permeation tube water bath temperature is 60°C; the reaction temperature is 50°C; the reaction time is 10min; the mass proportion of AC-FA and PY is 1:1.

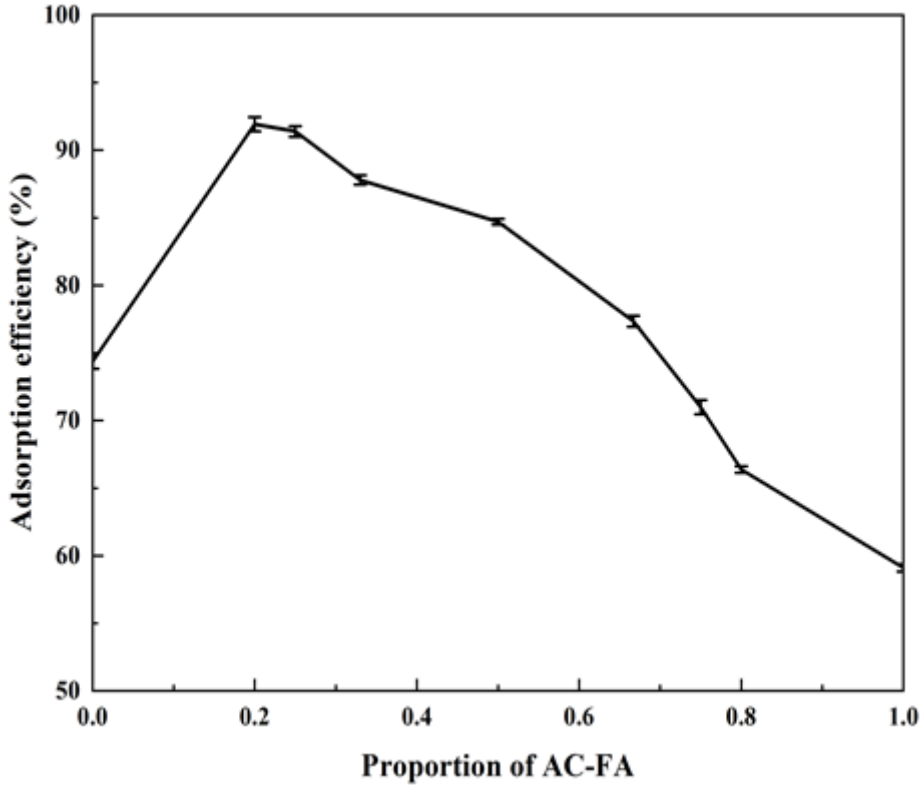

Figure 5

Influence of proportion of modified fly ash. Reaction conditions: the nitrogen flow rate is 1.2L/min; the mercury permeation tube water bath temperature is 60°C; the reaction time is 10min; the reaction temperature is 50°C.

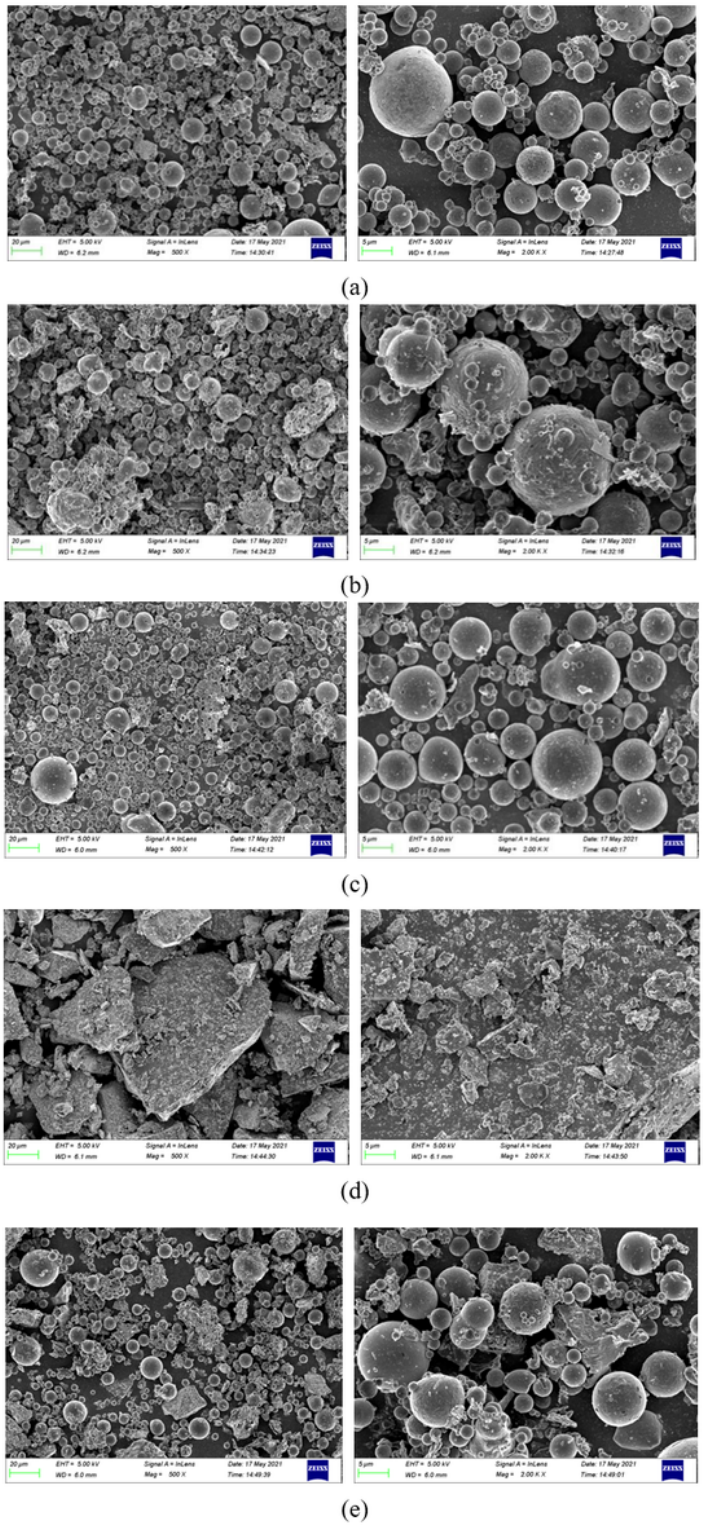

Figure 6

SEM characterization of samples

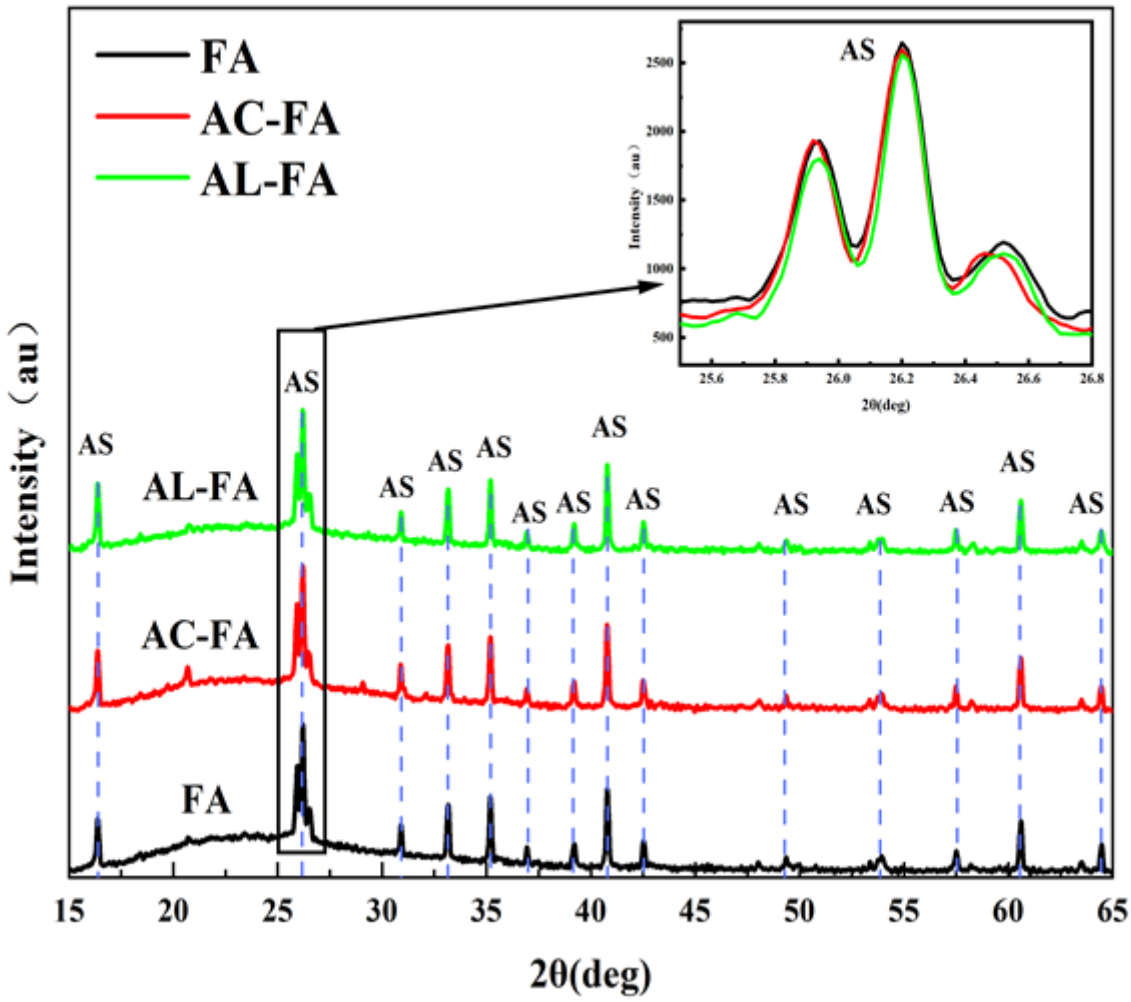

Figure 7

X-ray diffraction pattern of FA before and after modification.

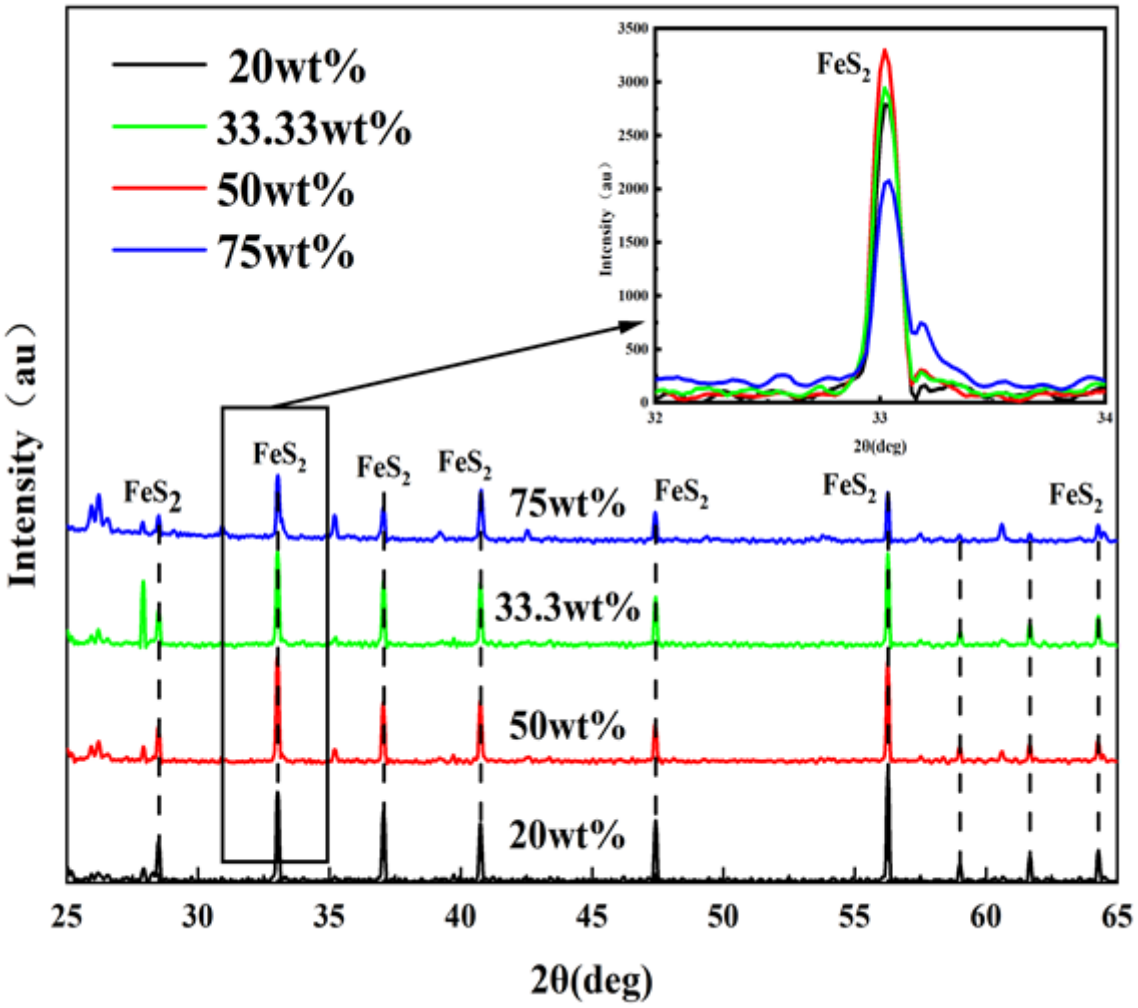

Figure 8

XRD patterns of adsorbents with different doping proportions

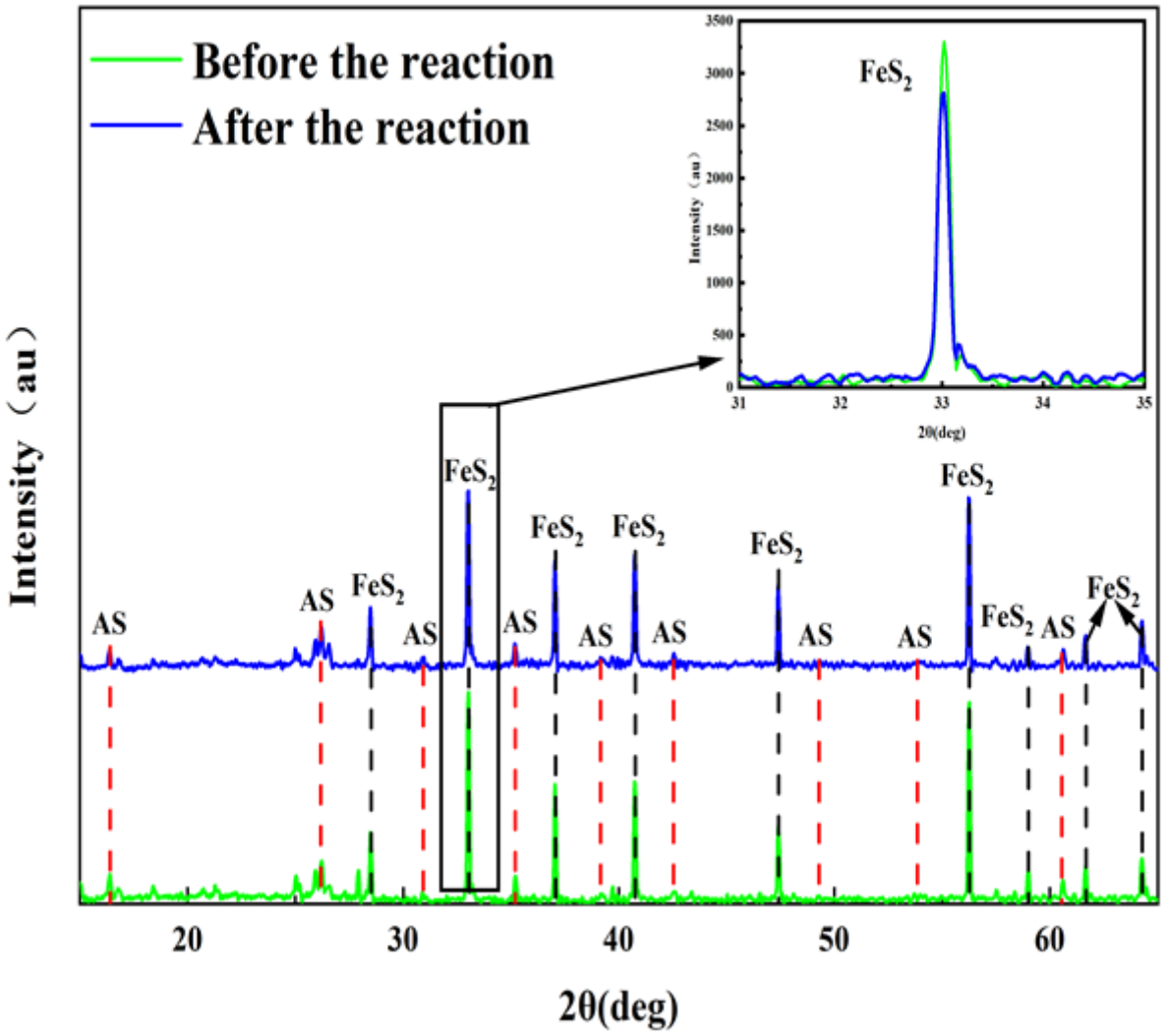

Figure 9

XRD images of adsorbent before and after reaction

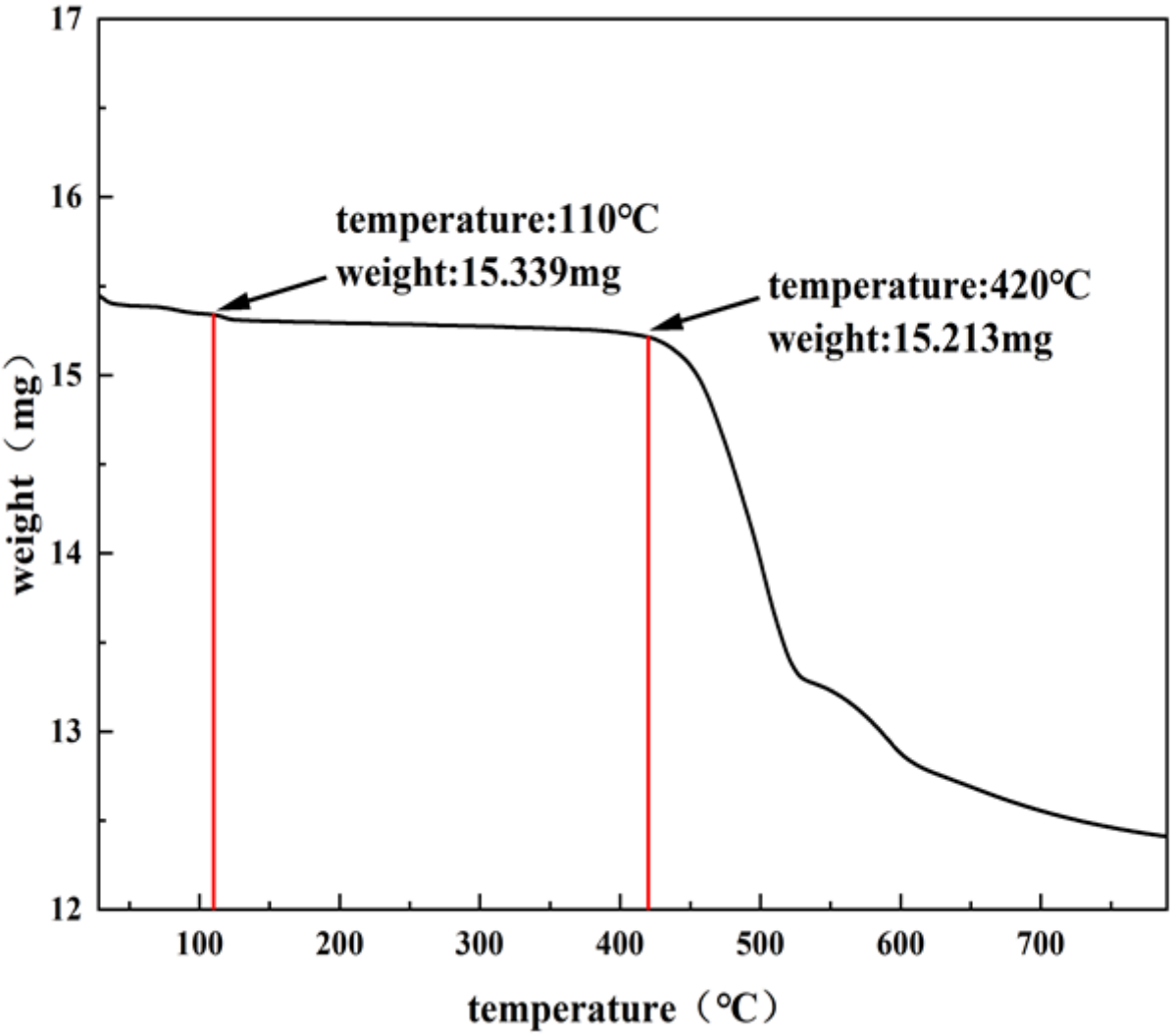

Figure 10

TG diagram of PY+AC-FA after reaction